

Energy Efficiency and Resource Allocation of IEEE 802.15.6 IR-UWB WBANs: Current State-of-the-Art and Future Directions

Yang Liu, Kemal Davaslioglu, and Richard D. Gitlin

Department of Electrical Engineering

University of South Florida

Email: yangl@mail.usf.edu, {kemald, richgitlin}@usf.edu

Abstract—Network life time of Wireless Body Area Network (WBANs) is essential for its operation. An integral part of the network life time is the energy efficiency of the devices and enabling their transmissions with the optimal choice of Physical layer (PHY) and Medium Access Control (MAC) parameters. Particularly, in the next generation wireless networks, where devices and sensors are heterogeneous and coexist in the same geographical area creating possible collisions and interference to each other, the battery power needs to be efficiently used. This paper consists of four complementing parts. In the first two parts, we study the two optimization algorithms proposed in our prior work. The first algorithm, Cross-Layer Optimization for Energy Efficiency (CLOEE), enables us to carry out a cross-layer resource allocation that addresses the rate and reliability trade-off in the PHY as well as the frame size optimization and transmission efficiency for the MAC layer. The second algorithm, Energy Efficiency Optimization of Channel Access Probabilities (EECAP), studies the case where the nodes access the medium in a probabilistic manner and jointly determines the optimal access probability and payload frame size for each node. These two algorithms address the problem from an optimization perspective. In the third part of the paper, we study the same problem from a game theoretical point of view. The last part of the paper is devoted to summarizing the challenges ahead and future research directions to increase the energy efficiency and network life time of WBANs.

I. INTRODUCTION

The recent advances in wireless sensor applications and wearable technologies enable the ubiquitous recording and pervasive health monitoring for the patients. These recordings can be complemented with the patient's medical history, genetic background, and personal habits to make better predictions about the patient's current health status. These recordings can be continuously sent to a cloud server for storage or to the medical doctors and/or emergency personnel for an immediate action. However, these life saving attributes are only possible if the limited resources of a wireless device are efficiently used. In 2012, IEEE finalized a standard for short-range and extreme low power communication to support the medical monitoring and personal entertainment applications under the IEEE 802.15.6 framework [1]. This standard considers three physical (PHY) layer methods as the narrowband PHY, ultra wideband (UWB) PHY, and human body communications PHY. In this paper, we focus on the UWB-PHY due to its

ultra-low power consumption, high data rate, and robustness against channel variations.

There are several methods to increase the energy efficiency of wireless sensor networks. First, link adaptation methods jointly optimize the PHY and medium access control (MAC) layer parameters [2], [3] and provide means to adapt the transmissions to the channel characteristics. Related works in [4]–[6] and our prior work in [2], [3] present different ways to implement link adaptation in WBANs. Second, introduction of sleeping patterns and duty cycling [7]–[9] offers significant energy savings to the wireless devices by turning off some of the energy-hungry components or the whole device itself periodically. This research area has been investigated widely in IEEE 802.15.6 through the m -periodic scheduled allocation mode [1], where the devices enter into sleep modes between superframes. The papers in [10]–[13] investigate this problem to determine the optimal m that maximizes the device life time taking into various constraints. The third method includes joint low duty cycle MAC and routing protocols that trade off latency, reliability, and energy efficiency [14]–[17] such that nodes wake up to transmit if they have data to transmit or they need to forward another node's traffic, while they sleep in the remaining periods. Although the duty cycling and sleep modes bring significant energy savings, the devices still need to wake-up periodically and monitor if there is a packet to be received or forwarded. The fourth method of integrating Wake-up Radio (WuR) transceivers to the main radio module addresses this problem so that the devices can wake-up on on-demand basis. When a WuR receives a Wake-up Call (WuC), it sends a message to the microcontroller to wake up the main radio's transceiver, while in the remaining times, only the WuR is awake and the remaining radio hardware is put to sleep.

In this paper, we summarize the two link adaptation and cross-layer optimization frameworks we proposed in [2], [3]. We formulate an energy efficiency maximization problem for the IEEE 802.15.6 IR-UWB PHY and propose a cross-layer optimization algorithm for energy efficiency (CLOEE) [2] to determine the optimal payload size in MAC layer and number of pulses per burst in physical layer. The algorithm has low complexity that owes it to the derived closed-form expressions. We note that prior work in this area has con-

sidered either optimization with respect to only one of the parameters and without addressing the rate constraints [4]–[6], or when they did, they relied on high complexity integer programming solutions for narrowband PHY and no closed-form expressions were obtained [10], [11]. Thus, CLOEE addresses the shortcomings the prior work and facilitates real-time link adaptation.

The second algorithm in this paper extends CLOEE and includes the random channel access probabilities of each node. We take into account the MAC layer collisions and derive the MAC layer successful transmission probabilities. The proposed algorithm, Energy Efficiency Optimization of Channel Access Probabilities (EECAP) [3], determines the optimal channel access probability and frame length that maximizes the energy efficiency of multiple sensors under the rate and access constraints. We note that the model in [4] takes the channel access probabilities into account, but does not provide an optimal distribution of access probabilities for multiple sensors and does not consider two or more parameters in their optimization. EECAP is proposed to address these shortcomings. To the best of our knowledge, the prior work in [2] and [3] are the first papers that determine the optimal frame size, modulation scheme, and channel access probability to maximize the network energy efficiency subject to the rate and channel access constraints. Furthermore, the proposed frameworks are general and can be applied to any protocol although we particularly employ the parameters of the IEEE 802.15.6 standard.

The rest of this paper is organized as follows. First, we provide an overview of the IEEE 802.15.6 standard in Section II. The first part of the paper in Section III describes the energy consumption model, formulates the energy efficiency maximization problem, and overviews the proposed link adaptation algorithm CLOEE. Section IV extends the problem formulation to include the channel access probabilities and the EECAP algorithm is presented. Section V discusses the game theoretical aspects of the network energy efficiency maximization problem. In Section VI, we provide a summary of lessons learned, the challenges that lie ahead, and discuss the future research directions.

II. SYSTEM MODEL

A. Overview of the IEEE 802.15.6 UWB PHY

The network topology we consider is a one-hop star network, which consists of multiple WBAN sensor nodes and a hub, whose function is medium access and power management. The hub can serve up to 64 nodes as shown in the standard [1]. The frequency spectrum is 3.1–10.6 GHz, which is divided into eleven channels. Each channel has a bandwidth of 499.2 MHz and there are three low band channels and eight high band channels. Three modulation schemes are supported in IR-UWB, namely on-off modulation, differential binary phase shift keying (DBPSK), and differential quadrature phase shift keying (DQPSK). Two modes of operation are defined in [1]. One is the default mode, which is for the medical and non-medical applications. The other is the high QoS mode,

which is used for high-priority medical applications only. In this paper, we only discuss the default mode due to the space limitation.

B. UWB PHY Superframe Structure

The UWB PHY frame format is referred to as the physical layer protocol data unit (PPDU). It consists of three parts: the synchronization header (SHR), the physical layer header (PHR), and the physical layer service data unit (PSDU). Therefore, the duration of the PPDU is $T_{\text{PPDU}} = T_{\text{SHR}} + T_{\text{PHR}} + T_{\text{PSDU}}$, where the frame durations for SHR, PHR, and PSDU are denoted by T_{SHR} , T_{PHR} , and T_{PSDU} , respectively.

The SHR frame consists of the preamble and the start-of-frame delimiter (SFD). The function of the preamble is used for timing synchronization, packet detection, and carrier frequency offset recovery. The preamble also enables the coexistence of WBANs [1]. The SFD is for frame synchronization. According to the SHR structure in [1], the SHR symbol shall use on-off keying (OOK) modulation with a zero-padding period of $L \cdot T_w = 128$ nsec. $L - 1 = 15$ zeros will be padded between the symbols and $T_w = 8$ nsec stands for the duration of a pulse waveform. The preamble and SFD are made up of four and one Kasami sequences of 63 bits, respectively. Therefore, the time duration of the SHR frame is $T_{\text{SHR}} = 5 \cdot 63 \cdot 128 \text{ nsec} = 40.32 \mu\text{sec}$.

The PHR frame consists of 24 bits that carry information about the data rate of the PSDU, MAC frame body length, pulse shape, burst mode, HARQ, and scrambler seed. A shortened Bose-Chaudhuri-Hocquenghem (BCH) code of $(n, k; t_{\text{ECC}}) = (40, 28; 2)$ is used, where n is the length of coded bits, k is the size of information bits and t_{ECC} means the error correcting capability. Hence, the PHR frame bits, $N_{\text{PHR}} = 40$, are transmitted at a sampling rate of 2051.2 nsec, i.e., $T_{\text{PHR}} = 40 \times 2051.3 \text{ nsec} = 82.052 \mu\text{sec}$.

For the default mode, the PSDU includes the MAC protocol data unit (MPDU) and the BCH parity bits. The MPDU consists of a MAC header, a variable length MAC frame body, and a frame check sequence (FCS). The header and FCS of the MPDU frame are $N_{\text{FCS}} = 56$ and $N_{\text{MH}} = 16$ bits, respectively. The MAC frame body has a variable length of N'_{FB} bits. Thus, in a MPDU frame, the total number of bits before bit stuffing are given as $N'_{\text{MPDU}} = N_{\text{MH}} + N_{\text{FCS}} + N'_{\text{FB}}$. For the PSDU frame, a BCH $(n = 63, k = 51; t_{\text{ECC}} = 2)$ code is used. The MPDU frame is grouped in blocks of length k to be encoded into codewords of length n after adding the parity bits. To align the symbol boundaries, bits are padded to the last word if $\text{rem}(N'_{\text{FB}} + 72, k) \neq 0$, where $\text{rem}(x, y)$ is the remainder of x divided by y . The duration of the PSDU frame is $T_{\text{PSDU}} = N_{\text{T}}/R_b$, where R_b is one of the uncoded bit rates in Table I of [2] and N_{T} is the PSDU frame size in bits. The problem formulations in Section III-B and IV-B will use the N_{T} to relate the error probability which depends on the number of codewords N_{CW} , which can be expressed as $N_{\text{CW}} = \frac{N_{\text{T}}}{n}$. Relating N_{CW} to N_{T} will help us derive the expressions in Section II-D.

C. Modulation, Receiver, and Probability of Bit Error

On-off modulation is a combination of M-ary waveform coding and on-off keying. With the on-off modulation, K bits from an alphabet size of $M = 2^K$ are grouped, $(b_0, b_1, \dots, b_{K-1})$, and passed through a symbol mapper of rate $1/2$ such that an output sequence of $2K$ bits, $(d_0, d_1, \dots, d_{2K-1})$, is obtained that has the same alphabet size.

In [1], $K = 1$ is considered as the default mode with an optional mode of $K = 4$. For example, the input bit 0 is mapped to $[1\ 0]$, while 1 is mapped to $[0\ 1]$. Each symbol contains one or multiple pulse waveforms. The symbol time T_{sym} has N_w pulse waveform positions each with a duration of T_w , so $T_{\text{sym}} = N_w T_w$. The symbol duration is divided into two intervals of duration $T_{\text{sym}}/2$ in order to enable on-off modulation. The duty cycle T_w/T_{sym} is fixed at $1/32 = 3.125\%$ in [1] to ensure low power consumption. The pulse waveform $w_n(t)$ is given by $w_n(t) = \sum_{i=0}^{N_{\text{cpb}}-1} (1 - 2s_i)p(t - iT_p)$, where $p(t)$ denotes a single pulse of duration T_p [1].

The sequence $\{s_i\}$ denotes the scrambling sequence that helps reduce the spectral lines due to same polarity pulses [1], [18]. The integer N_{cpb} defines the number of pulses per burst and $N_{\text{cpb}} \geq 1$. In the single pulse case, $N_{\text{cpb}} = 1$, whereas $N_{\text{cpb}} \in \{2, 4, 8, 16, 32\}$ for the burst pulse option. Note that the processing gain of an IR-UWB system is $N_{\text{cpb}} N_w$ [18]. Because $N_w = 32$ is fixed by the standard [1], the processing gain can be varied by changing N_{cpb} .

A non-coherent detector is considered and equally likely input bits are assumed. Each pulse has an energy of $\varepsilon_p = \varepsilon_b/N_{\text{cpb}}$. The bit error probability is given by [4], [19]

$$P_b = Q\left(\sqrt{\frac{1}{2} \cdot \frac{(h\varepsilon_b/N_0)^2}{h\varepsilon_b/N_0 + N_{\text{cpb}}T_{\text{int}}W_{\text{rx}}}}\right), \quad (1)$$

where h is the channel coefficient, T_{int} is the integration interval per pulse, W_{rx} is the equivalent noise bandwidth of the receiver front end, and ε_p/N_0 is the integrated signal-to-noise ratio per bit. In our simulations, we take the integration time as the pulse duration, i.e., $T_{\text{int}} = N_{\text{cpb}}T_p$, and assume that the receiver and transmitter are fully synchronized.

D. Error Correction

In Section II-B, we discussed the structure of an UWB frame that consists of SHR, PHR, and PSDU, and determined the time duration for each type of frame. In Section II-C, the bit error probability is presented for a non-coherent ED receiver. In what follows, we discuss the error correcting capabilities of each frame type.

The SHR frame is correctly received at the receiver if both the preamble and the SFD transmissions are successful, which can be mathematically expressed as $P_{\text{SHR}} = P_{\text{SFD}}P_{\text{Preamble}}$, where P_{SFD} and P_{Preamble} are the probabilities of correctly decoding the SFD and preamble frame, respectively. Since there are one and four Kasami sequences in the SFD and preamble, we have $P_{\text{Preamble}} = (1 - P_{\text{Kasami}})^4$ and $P_{\text{SFD}} = P_{\text{Kasami}}$. The probability of successful delivery of a 63-bit Kasami sequence

can be expressed as $P_{\text{Kasami}} = \sum_{i=0}^{\rho} \binom{63}{i} (P_b)^i (1 - P_b)^{63-i}$, where the operator $\binom{a}{b}$ represents the binomial coefficient and ρ is an implementation-dependent sensitivity margin and it is taken as $\rho = 6$ [3].

The BCH decoder can recover up to t_{ECC} bit errors for a $\text{BCH}(n, k; t_{\text{ECC}})$ code. Then, the probability of successful reception of the PHR frame is [20]

$$P_{\text{PHR}} = \sum_{i=0}^{t_{\text{ECC}}} \binom{N_{\text{PHR}}}{i} (P_b)^i (1 - P_b)^{N_{\text{PHR}}-i}, \quad (2)$$

where $N_{\text{PHR}} = 40$ bits, $t_{\text{ECC}} = 2$ and P_b is given in (1).

The PSDU frame consists of N_{CW} codewords. Let P_{CW} denote the probability of successfully receiving of a codeword, which can be expressed as

$$P_{\text{CW}} = \sum_{i=0}^t \binom{n}{i} (P_b)^i (1 - P_b)^{n-i}. \quad (3)$$

Then, the PSDU frame is received correctly if all the codewords are received successfully as

$$P_{\text{PSDU}} = (P_{\text{CW}})^{N_{\text{CW}}} = (P_{\text{CW}})^{\frac{N_T}{n}}. \quad (4)$$

The probability of successful delivery of the whole PPDU superframe is when the SHR, PHR, and PSDU frames are successfully received, at the same time, that is

$$P_{\text{PPDU}} = P_{\text{SHR}} P_{\text{PHR}} P_{\text{PSDU}} = P_{\text{SHR}} P_{\text{PHR}} (P_{\text{CW}})^{\frac{N_T}{n}} \quad (5)$$

where P_{SHR} , P_{PHR} , and P_{PSDU} are the successful delivery probabilities of the each frame type, respectively. For the default mode, $n = 63$ is the length of coded bits of a codeword. There is a trade-off between system efficiency and error probability. A short N_T will result in a poor performance due to high packet overhead but if there error probability is high, that should be the preferred solution, whereas a higher N_T will provide a higher system efficiency (in terms of throughput and energy efficiency) if the frame error probability is low.

III. CLOEE: CROSS-LAYER OPTIMIZATION FOR ENERGY EFFICIENCY

A. Energy Consumption Model

The energy of a device is consumed by different hardware components, e.g., the analog-to-digital converter (ADC), the power amplifier (PA), low-noise amplifier (LNA), demodulator, clock generator, synchronizer, variable gain amplifier (VGA), the pulse generator, etc. There are several models in the literature that characterize the energy consumption of IR-UWB radios, e.g., [4], [5], [21], [22]. In this paper, we employ the model in [21] due to its wide applicability that accommodates the coherent and non-coherent detectors, hard and soft decision demodulators, and different modulation types. The energy required to transmit and receive a payload bit as given by [21]

$$\varepsilon_B = (\varepsilon_{\text{FB}}^{\text{Tx}} + \varepsilon_{\text{FB}}^{\text{Rx}})/N_T, \quad (6)$$

where $\varepsilon_{\text{FB}}^{\text{Tx}}$ and $\varepsilon_{\text{FB}}^{\text{Rx}}$ represent the energy consumed at the transmitter and receiver for the PSDU frame, respectively. These two terms can be further expressed as

$$\begin{aligned}\varepsilon_{\text{FB}}^{\text{Tx}} &= \varepsilon_p N_{\text{cpb}} N_T + P_{\text{SYN}} T_{\text{onL}}, \\ \varepsilon_{\text{FB}}^{\text{Rx}} &= (M P_{\text{COR}} + \rho_c P_{\text{ADC}} + P_{\text{LNA}} + P_{\text{VGA}} + \rho_r (P_{\text{GEN}} + P_{\text{SYN}})) T_{\text{onL}},\end{aligned}\quad (7)$$

where P_{SYN} is the power consumption of the clock generator and synchronizer at the transmitter and T_{onL} is the time duration to transmit N_T bits, $T_{\text{onL}} = T_{\text{sym}} N_T$. The terms P_{COR} , P_{ADC} , P_{LNA} , P_{VGA} , and P_{GEN} , respectively, represent the power consumption of the RAKE fingers of the receiver, the ADC, LNA, VGA, and pulse generator. The number of RAKE receiver fingers is denoted by M . For coherent modulation, ρ_r takes the value one and for non-coherent modulation, ρ_r is zero. For soft decision, ρ_c is one, whereas ρ_c is zero for hard decision.

Similarly, the overhead energy consumption is defined as $\varepsilon_{\text{OH}} = \varepsilon_{\text{OH}}^{\text{Tx}} + \varepsilon_{\text{OH}}^{\text{Rx}}$, where $\varepsilon_{\text{OH}}^{\text{Tx}}$ and $\varepsilon_{\text{OH}}^{\text{Rx}}$ denote the energy to transmit and receive the overhead, respectively, and these are

$$\begin{aligned}\varepsilon_{\text{OH}}^{\text{Tx}} &= (N_{\text{cpb}}^{\text{SHR}} N_{\text{SHR}} + N_{\text{cpb}}^{\text{PHR}} N_{\text{PHR}}) \varepsilon_p + P_{\text{SYN}} (T_{\text{SHR}} + T_{\text{PHR}}), \\ \varepsilon_{\text{OH}}^{\text{Rx}} &= (M P_{\text{COR}} + \rho_c P_{\text{ADC}} + P_{\text{LNA}} + P_{\text{VGA}} \\ &\quad + \rho_r (P_{\text{GEN}} + P_{\text{SYN}})) (T_{\text{SHR}} + T_{\text{PHR}}),\end{aligned}\quad (8)$$

where $N_{\text{cpb}}^{\text{SHR}} = 4$, $N_{\text{cpb}}^{\text{PHR}} = 32$, $N_{\text{SHR}} = 63 \cdot 5 = 315$, and T_{SHR} and T_{PHR} are defined as in Section II-B.

Finally, the startup energy is $\varepsilon_{\text{ST}} = \varepsilon_{\text{ST}}^{\text{Tx}} + \varepsilon_{\text{ST}}^{\text{Rx}} = 2 P_{\text{SYN}} T_{\text{ST}}$, where T_{ST} is the time duration for the start up of the devices.

B. Problem Formulation

In the network model, we consider one-hop star topology where N_S nodes communicate to a hub as illustrated in Fig. 1. Without loss of generality, we assume that each node requests R_0 bits per second. We first make the definitions of energy efficiency and throughput, and then formulate the problems. The energy efficiency can be defined as the ratio of the total number of successfully received bits to the total energy consumed at the transmitter and receiver with the units of bits/Joule. It can be mathematically expressed as [2]

$$\eta(N_T, N_{\text{cpb}}) = \frac{N_T P_{\text{SHR}} P_{\text{PHR}} (P_{\text{CW}})^{\frac{N_T}{n}}}{N_T \cdot \varepsilon_B + \varepsilon_{\text{OH}} + \varepsilon_{\text{ST}}}. \quad (9)$$

When we take the derivative of (9) with respect to N_T and rearrange the terms, we obtain [2]

$$N_T^{\text{EE}} = \left[\sqrt{\frac{(\varepsilon_{\text{OH}} + \varepsilon_{\text{ST}})^2}{(2\varepsilon_B)^2} - \frac{n(\varepsilon_{\text{OH}} + \varepsilon_{\text{ST}})}{\varepsilon_B \log(P_{\text{CW}})}} - \frac{\varepsilon_{\text{OH}} + \varepsilon_{\text{ST}}}{2\varepsilon_B} \right]. \quad (10)$$

It is shown in [2] that energy efficiency is strictly quasiconcave in N_T . Since η is a strictly quasiconcave, a local optimal solution is also a global maximum solution [23].

Similarly, we can define the network throughput as the ratio of the total number bits that are successfully received at receiver to the duration of a frame, which is in the units of

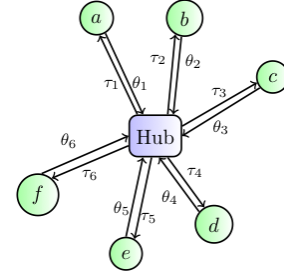


Figure 1. One-hop WBAN star network topology consisting of multiple nodes and a hub. Nodes send their application requirements and the hub sends back their MAC and PHY layer assignments.

bits/sec. It can be expressed as

$$R(N_T, N_{\text{cpb}}) = \frac{N_T P_{\text{SHR}} P_{\text{PHR}} (P_{\text{CW}})^{\frac{N_T}{n}}}{T_{\text{SHR}} + T_{\text{PHR}} + N_T T_{\text{sym}}}, \quad (11)$$

where the terms P_{SHR} and P_{PHR} are functions of N_{cpb} through P_b . The probability P_{CW} is a function of both N_T and N_{cpb} . By following the same steps as in (10), the optimal PSDU frame size that maximizes the throughput for a given N_{cpb} is

$$N_T^{\text{THR}} = \left[\sqrt{\frac{(T_{\text{SHR}} + T_{\text{PHR}})^2}{(2T_{\text{sym}})^2} - \frac{n(T_{\text{SHR}} + T_{\text{PHR}})}{T_{\text{sym}} \log(P_{\text{CW}})}} - \frac{T_{\text{SHR}} + T_{\text{PHR}}}{2T_{\text{sym}}} \right]. \quad (12)$$

We formulate the network energy efficiency maximization problem subject to the minimum rate constraint as

$$\begin{aligned}(\mathbf{P}) \quad \max \quad & \frac{f(N_T, N_{\text{cpb}})}{g(N_T, N_{\text{cpb}})} = \frac{N_T P_{\text{SHR}} P_{\text{PHR}} (P_{\text{CW}})^{\frac{N_T}{n}}}{(N_T \varepsilon_B + \varepsilon_{\text{OH}} + \varepsilon_{\text{ST}})} \\ \text{s.t.} \quad & \frac{N_T P_{\text{SHR}} P_{\text{PHR}} (P_{\text{CW}})^{\frac{N_T}{n}}}{T_{\text{SHR}} + T_{\text{PHR}} + T_{\text{sym}} N_T} \geq R_0 N_S.\end{aligned}\quad (13)$$

To solve the above problem, the Lagrangian of (13) can be expressed as

$$\mathcal{L}(N_T, N_{\text{cpb}}, \lambda) = \eta(N_T, N_{\text{cpb}}) + \lambda (R(N_T, N_{\text{cpb}}) - R_0 N_S), \quad (14)$$

where λ is the Lagrangian variable associated with the minimum rate constraints. Since the problem (13) is a single-ratio fractional program, we can solve it by its solving the dual fractional program [2]. Let $h(N_T, N_{\text{cpb}})$ denote

$$h(N_T, N_{\text{cpb}}) = R_0 N_S - \frac{N_T P_{\text{SHR}} P_{\text{PHR}} (P_{\text{CW}})^{\frac{N_T}{n}}}{T_{\text{SHR}} + T_{\text{PHR}} + T_{\text{sym}} N_T}. \quad (15)$$

Then, the dual fractional program can be expressed as [2]

$$(\mathbf{D}) \quad \min_{\lambda \geq 0} \left[\max_{N_T} \frac{f(N_T, N_{\text{cpb}}) - \lambda h(N_T, N_{\text{cpb}})}{g(N_T, N_{\text{cpb}})} \right]. \quad (16)$$

Problem (16) can be solved iteratively. First, λ is fixed and (16) is solved using any line search method, and N_T^* is obtained. Next, the dual variable λ is updated using

$$\lambda_{l+1} = [\lambda_l - \alpha_l (R(N_T^*, N_{\text{cpb}}) - R_0 N_S)]^+, \quad (17)$$

Algorithm 1 CLOEE – Cross-Layer Optimization for Energy Efficiency for IEEE 802.15.6 IR-UWB

```

1: function CLOEE( $\varepsilon_B, \varepsilon_{OH}, \varepsilon_{ST}, T_{SHR}, T_{PHR}, T_p, R_0, N_S$ )
2:   Set an all-zeros vector  $\mathbf{N}_T$  of size  $|\{N_{cpb}\}|$  and  $n \leftarrow 0$ 
3:   for  $N_{cpb} = \{1, 2, 4, 8, 16, 32\}$  do
4:     Set  $l \leftarrow 0$  and solve (10) to obtain  $N_T(l)$ 
5:     Set  $\lambda(l) \leftarrow \max(R_0 N_S - R(N_T(l), N_{cpb}(n)), 0)$ 
6:     if  $R(N_T(l), N_{cpb}(n)) \geq R_0 N_S$  then
7:        $N_T(n) \leftarrow N_T(l)$ 
8:     else
9:       if  $R(N_T^{THR}, N_{cpb}(n)) > R_0 N_S$  then
10:        repeat
11:          Solve (16) to obtain  $N_T(l)$ 
12:          Update  $\lambda(l+1)$  using (17)
13:          Set  $l \leftarrow l+1$ 
14:        until stopping criteria is satisfied
15:         $N_T(n) \leftarrow N_T(l)$ 
16:       else
17:         $N_T(n) \leftarrow N_T^{THR}$ 
18:       end if
19:     end if
20:      $n \leftarrow n+1$ 
21:   end for
22:    $(N_T^*, N_{cpb}^*) \leftarrow \arg \max_{(N_T, N_{cpb})} \eta(N_T, N_{cpb})$ 
23: end function

```

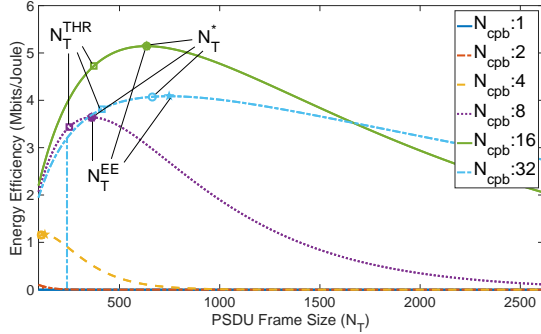


Figure 2. Energy efficiency and throughput versus the PSDU frame size at 8.4 meters for $R_0 = 15$ kbits/sec and $N_S = 24$ nodes.

where the operator $[x]^+$ denotes $\max(x, 0)$ and α_l is the step size of the l th iteration. The steps in (16) and (17) are iterated until the relative change in N_T between two iterations is less than some tolerance, i.e., $|N_T(l+1) - N_T(l)|/N_T(l) \leq \Delta$ [23].

We summarize CLOEE [2] under the heading Algorithm 1. Three cases are identified based on the link distances. First, for short to medium link distances where the throughput at N_T^{EE} satisfies the rate constraint, i.e., $R(N_T^{EE}, N_{cpb}^*) > R_0 N_S$, then N_T^{EE} is obtained in a single-step using (10). Second case typically occurs during the mode transitions such that the throughput at N_T^{EE} does not satisfy the rate constraint, but N_T^{THR} satisfies it, i.e., $R(N_T^{EE}) < R_0 N_S$ and $R(N_T^{THR}) > R_0 N_S$. In this case, we solve (16). The third case is for long link distances, where there is no N_T that satisfies the rate constraint at N_{cpb} , then N_T^{THR} is chosen as N_T . We illustrate

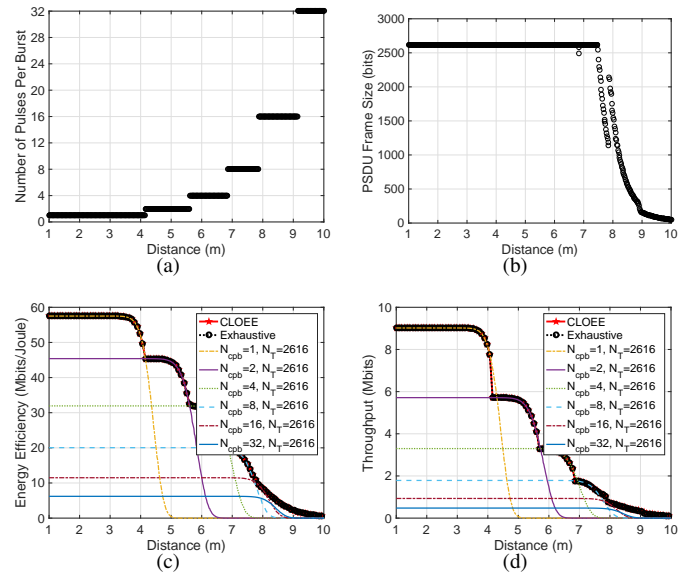


Figure 3. Link adaptation results for maximizing the energy efficiency.

the dependence of the energy efficiency on the PSDU frame size in Fig. 2. The critical points of N_T^{EE} , N_T^{THR} , and N_T^* are also shown. These figures also confirm the quasiconcave nature of η . Note that the order of these curves closely depends on the link distances, see Figs. 3(c)-(d).

C. Link Adaptation Results

In this subsection, we evaluate the performance of CLOEE and compare it to several static strategies. We consider the channel model in [24] to characterize the propagation environment in the 3.1-10.6 GHz band. The path loss model is taken as $L(d) = a \cdot \log_{10}(d) + b + \chi$, where a and b are constants, d is the distance in millimeters, and χ is a Gaussian distributed random variable with a zero mean and a variance σ^2 . Typical values for a hospital room are $a = 19.2$, $b = 3.38$, and $\sigma = 4.40$ [24]. The noise spectral density is taken as -174 dBm/Hz, W_{rx} as 499.2 MHz, noise figure as 10 dB, and implementation margin as 5 dB [1]. A non-coherent receiver and hard decision combining is considered, $\rho_r = 0$, and $\rho_c = 0$. For the energy consumption model, we have $\varepsilon_p = 20$ pJ, $P_{COR} = 10.08$ mW, $P_{ADC} = 2.2$ mW, $P_{LNA} = 9.4$ mW, $P_{VGA} = 22$ mW, $P_{SYN} = 30.6$ mW, $P_{GEN} = 2.8$ mW, and $T_{ST} = 400$ μ s [21].

Link adaptation results are presented in Figs. 3(a)-(d) as link distance varies between one to ten meters. The performance of different PSDU frame size and the number of pulses per burst are depicted. The results obtained using CLOEE are presented in Figs. 3(a)-(b). We observe that longer frame sizes and higher data rates (few pulses per burst) provide the highest energy efficiency for distances up to 7.5 meters. For link distances beyond this point, the SNR becomes low and higher error probabilities occur so that shorter frames sizes and more pulses per burst need to be employed in order to maintain the link reliability. In Figs. 3(c)-(d), the performance of five static strategies, exhaustive search, and CLOEE are evaluated. The

performance of CLOEE and exhaustive search overlap which demonstrates the advantage of CLOEE as its computational complexity is much smaller. As expected, CLOEE outperforms the static strategies in various performance metrics. The energy efficiency and throughput performance versus reliability can again be observed in Figs. 3(c)-(d). For example, the point $(N_{\text{cpb}}, N_{\text{T}}) = (1, 2616)$ provides very high energy efficiency and throughput at distances less than 4 meters, whereas its link reliability is very low. The reliable point $(N_{\text{cpb}}, N_{\text{T}}) = (32, 2616)$ provides a very robust transmission, while it is highly inefficient at short distances.

IV. EECAP: ENERGY EFFICIENCY OPTIMIZATION OF CHANNEL ACCESS PROBABILITIES

Consider the scenario where each node contends to access the channel and the hub works as a controller to determine the optimal access probability of the nodes. Fig. 1 depicts an example scenario where multiple nodes report their requirements, denoted by θ_k , and the hub assigns their channel access probabilities. We can consider several application related requirements that can be represented by multi-bit signals and encompass a variety of constraints such as the rate, delay, power, reliability, QoS, and security levels. In this paper, we only consider the minimum rate constraint for simplicity, i.e., $\theta_k = R_k^{\min}$, although extensions to multiple constraints is straightforward.

A. Incorporating Channel Access Probabilities

In this part, we identify three channel states and derive the expressions for their probabilities, time duration, and energy consumption at these channel states.

- 1) **Successful transmission:** The probability of successful transmission of node k can be expressed as

$$P_k^S = \tau_k \prod_{j \neq k} (1 - \tau_j) = \tau_k (1 - p_k), \quad (18)$$

where $p_k = 1 - \prod_{j \neq k} (1 - \tau_j)$ is the collision probability experienced by node k due to other nodes [25]. Then, the probability of successful transmission for all the nodes is

$$P^S = \sum_k P_k^S = \sum_k \tau_k (1 - p_k). \quad (19)$$

For a node k , the time it takes to successfully transmit its packet and receive its acknowledgment from the hub can be expressed as

$$T_k^S = T_k^{\text{PPDU}} + T_{\text{ACK}} + 2T_{\text{pSIFS}} + 2\sigma_k, \quad (20)$$

where $T_k^{\text{PPDU}} = T_{\text{SHR}} + T_{\text{PHR}} + N_k^T T_{\text{sym}}$ is PPDU time duration of node k , which has been defined in Section II-B. The time duration of the acknowledgment (ACK) packet from the hub is $T_{\text{ACK}} = T_{\text{SHR}} + T_{\text{PHR}} + N_{\text{T}}^{\text{ACK}} T_{\text{sym}}$, where we assume the ACK packet is $N_{\text{T}}^{\text{ACK}} = 126$ bits. The short interframe spacing is $T_{\text{pSIFS}} = 75 \mu\text{sec}$ [1]. The propagation time is denoted by σ_k . For a successful transmission, the energy consumption can be written as $\varepsilon_k^S = \varepsilon_{\text{B}} N_k^T + \varepsilon_{\text{OH}} + \varepsilon_{\text{ST}}$, where ε_{B} stands for the energy

required to transmit and receive a payload bit, ε_{OH} is the energy consumption for the transmission and reception of the overhead, and ε_{ST} denotes the startup energy.

- 2) **Idle Channel:** The probability that a channel is idle is $P^I = \prod_k (1 - \tau_k)$. It takes $T_k^I = 292 \mu\text{sec}$ for the idle channel state as a CSMA slot time period [1]. When the channel is idle, we assume that no energy is consumed, i.e., $\varepsilon_k^I = 0$ [21].
- 3) **Collision:** More than one user tries to access the channel to transmit packets. This case occurs with probability $P^C = 1 - P^S - P^I$. The time spent at the collision channel state can be expressed as $T_k^C = T_k^{\text{PPDU}} + T_{\text{pSIFS}} + \sigma_k$. The energy consumed during the collision state is $\varepsilon_k^C = \varepsilon_{\text{B}}^{\text{Tx}} N_k^T + \varepsilon_{\text{OH}}^{\text{Tx}} + \varepsilon_{\text{ST}}^{\text{Tx}}$, where $\varepsilon_{\text{B}}^{\text{Tx}}$, $\varepsilon_{\text{OH}}^{\text{Tx}}$, and $\varepsilon_{\text{ST}}^{\text{Tx}}$ are defined similarly as the energy required for payload bit, overhead, and startup in transmission only.

B. Problem Formulation

The energy efficiency and throughput definitions that include the channel access probabilities need to be updated. The energy efficiency of node k is the successfully transmitted payload information divided by the average energy consumption, which can be expressed as

$$\eta_k = \frac{N_k^T P_k^S P_k^{\text{SHR}} P_k^{\text{PHR}} (P_k^{\text{CW}})^{\frac{N_k^T}{n}}}{P^S \varepsilon_k^S + P^C \varepsilon_k^C + P^I \varepsilon_k^I}. \quad (21)$$

Similarly, the throughput of node k is defined as the number of successfully transmitted payload bits divided by the average time duration, that is,

$$R_k = \frac{N_k^T P_k^S P_k^{\text{SHR}} P_k^{\text{PHR}} (P_k^{\text{CW}})^{\frac{N_k^T}{n}}}{P^S T_k^S + P^C T_k^C + P^I T_k^I}. \quad (22)$$

The minimum value of τ_k that satisfies the rate constraint can be obtained by letting $R_k = R_k^{\min}$ and rearranging terms to obtain [3]

$$\tau_{k,\min}^{\text{THR}} = \frac{R_k^{\min} \cdot YT}{N_k^T (1 - p_k) P_k^{\text{SHR}} P_k^{\text{PHR}} (P_k^{\text{CW}})^{\frac{N_k^T}{n}} - R_k^{\min} \cdot XT}, \quad (23)$$

where $XT = x_k^S T_k^S + x_k^C T_k^C + x_k^I T_k^I$ and $YT = y_k^S T_k^S + y_k^C T_k^C + y_k^I T_k^I$. If $\tau_{k,\min}^{\text{THR}} \notin (0, 1)$, there is no feasible solution for τ_k that satisfies the rate constraint. Then, the optimal PSDU frame length for the node k 's throughput is given by [3]

$$N_{k,T}^{\text{THR}} = \left\lceil -\frac{[n + \log(P_k^{\text{CW}})] \cdot TO}{\log(P_k^{\text{CW}}) \cdot TN} \right\rceil_{N_{\text{T}}^{\min}}^{N_{\text{T}}^{\max}}, \quad (24)$$

where $TO = P^S (T_{\text{SHR}} + T_{\text{PHR}} + T_{\text{ACK}} + 2T_{\text{pSIFS}} + 2\sigma_k) + P^C (T_{\text{SHR}} + T_{\text{PHR}} + T_{\text{pSIFS}} + \sigma_k) + P^I T_k^I$ and $TN = (P^S + P^C) T_{\text{sym}}$. The notation $[x]_a^b$ denotes that x is lower bounded by a and upper bounded by b . If $P_k^{\text{CW}} = 0$, then the throughput is always zero. If $P_k^{\text{CW}} = 1$, then $N_{k,T}^{\text{THR}} = N_{\text{T}}^{\max}$.

The problem (EE) maximizes the network energy efficiency subject to the minimum rate constraint and the access proba-

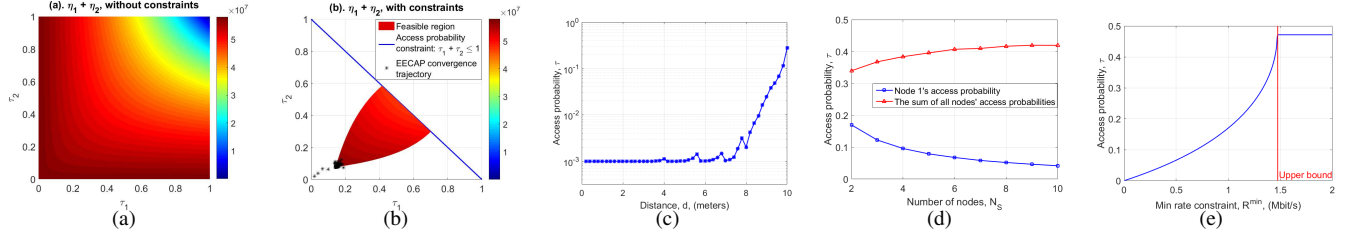


Figure 4. (a)-(b) Feasibility region of the (EE) problem with and without constraints where the link distances are 1 meter and $R_{min} = 1$ Mbits/sec for node 1 and 0.5 Mbits/sec for node 2. The optimal access probabilities versus the link distance (c), the number of nodes (d) and different values of minimum rate constraints (e) are depicted. The minimum rate constraint is taken as 1 Mbits/s. Link distance is 1 meter for (b) and (c). There are two nodes in (a) and (c).

Algorithm 2 EECAP: Energy Efficiency Optimization of Channel Access Probabilities [3]

```

1: Given  $d, h, R^{\min}$ , and  $N_S$ 
2: Initialize  $\tau$  and  $N_T$ 
3: repeat
4:   for node  $k = \{1, 2, \dots, N_S\}$  do
5:     solve (23) to obtain  $\tau_{k,\min}^{\text{THR}}$ 
6:     solve (24) to obtain  $N_{k,T}^{\text{THR}}$ 
7:   end for
8: until stopping criteria is satisfied
9: if  $R_k(\tau_{k,\min}^{\text{THR}}, N_{k,T}^{\text{THR}}) \geq R_k^{\min}$  and  $\sum_k \tau_{k,\min}^{\text{THR}} \leq 1$  then
10:  repeat
11:    for node  $k = \{1, 2, \dots, N_S\}$  do
12:      solve (27) to obtain  $(\tau_k)^{\text{EE}}$  and  $(N_k^T)^{\text{EE}}$ 
13:       $\lambda_k = \max(R_k^{\min} - R_k(\tau_k^{\text{EE}}, N_k^{\text{EE}}), 0)$ 
14:    end for
15:     $\mu^{\text{EE}} = \max(\sum_k (\tau_k)^{\text{EE}} - 1, 0)$ 
16:  until stopping criteria is satisfied
17:  return  $(\tau^*, N_T^*) = (\tau^{\text{EE}}, N_T^{\text{EE}})$ 
18: else
19:  repeat
20:    for node  $k = \{1, 2, \dots, N_S\}$  do
21:      solve (28) to obtain  $(\tau_k)^{\text{LogTHR}}$  and  $(N_k^T)^{\text{LogTHR}}$ 
22:    end for
23:     $\mu^{\text{LogTHR}} = \max(\sum_k (\tau_k)^{\text{LogTHR}} - 1, 0)$ 
24:  until stopping criteria is satisfied
25:  return  $(\tau^*, N_T^*) = (\tau^{\text{LogTHR}}, N_T^{\text{LogTHR}})$ 
26: end if

```

bility constraint, which can be formulated as

$$(\text{EE}) \quad \max \quad \sum_k \eta_k \quad (25a)$$

$$\text{s.t.} \quad R_k \geq R_k^{\min} \text{ for all } k \quad (25b)$$

$$\sum_k \tau_k \leq 1, \quad 0 \leq \tau_k \leq 1 \text{ for all } k \quad (25c)$$

$$N_T^{\min} \leq N_k^T \leq N_T^{\max} \text{ for all } k. \quad (25d)$$

The Lagrangian of (25) can be written as

$$\mathcal{L} = \sum_k \eta_k + \sum_k \lambda_k (R_k - R_k^{\min}) + \mu \left(1 - \sum_k \tau_k \right), \quad (26)$$

where λ_k is the Lagrangian variable associated with the minimum rate constraint of node k and μ is the Lagrangian variable related to the access probability constraint. The channel access

probability and the PSDU frame length for all the nodes are represented by the vectors $\tau = [\tau_1, \tau_2, \dots, \tau_{N_S}]$ and $N_T = [N_1^T, N_2^T, \dots, N_{N_S}^T]$, respectively, where the symbols in bold define vectors. The optimal solution, (τ^*, N_T^*) , as well as the corresponding Lagrangian variables $\lambda^* = [\lambda_1^*, \lambda_2^*, \dots, \lambda_{N_S}^*]$ and μ^* can be obtained by applying the Karush-Kuhn-Tucker (KKT) optimality conditions [23]. We solve the dual of (EE) problem using the Gauss-Seidel iterative method [3] as

$$(\text{Dual-EE}) \quad \min_{\lambda, \mu \geq 0} \left[\max_{\tau, N_T} \mathcal{L} \right]. \quad (27)$$

If there is no feasible solution for the (EE) problem, we replace its objective with the sum of the logarithm of energy efficiencies, that is,

$$(\text{LogTHR}) \quad \max_{\tau, N_T} \left(\sum_k \log R_k \right), \quad (28)$$

subject to (25c)-(25d).

The proposed algorithm in [3] is presented under the heading Algorithm 2. It has two stages. In the first stage, the feasibility of the problem is checked. We solve (23) and (24) to determine $\tau_{k,\min}^{\text{THR}}$ and $N_{k,T}^{\text{THR}}$. In the next stage, if these values satisfy the check conditions in (Step 9), then we solve (26) using dual decomposition method (Steps 10-17). If the problem does not have a feasible solution that satisfies the rate and access constraints, then we solve the (LogTHR) problem (Steps 19-25). Thus, the (LogTHR) problem is typically solved for high rate constraints or large link distances.

C. Simulation Results with Channel Access Probabilities

In what follows, the performance of the algorithm EECAP is evaluated and insights on what affects the network parameters are provided. The parameters are used as in Section III-C. The value of N_{cpb} is determined according to Fig. 3(a).

Figs. 4(a)-(b) illustrate the feasible regions of Problem (EE) with and without rate constraints, respectively. For visual clarity, we present the results for only two nodes. Since the energy consumption at the idle channel state is zero, the maximum energy efficiency is obtained when either node's access probability is zero, which is an unfair outcome. The trajectory of the EECAP solutions are shown with asterisk, which demonstrates its rapid convergence. After about 5 iterations, the algorithm steps into the feasible region and seeks

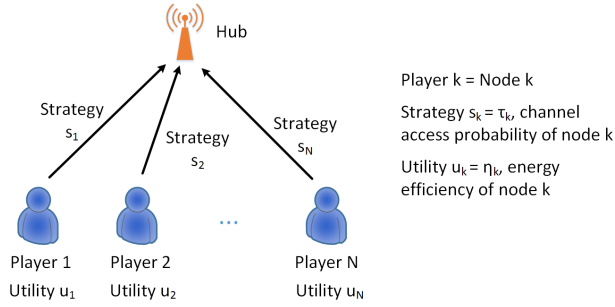


Figure 5. Energy Efficiency game in IEEE 802.15.6 UWB WBANs.

for the optimal solution that maximizes the sum of energy efficiencies. The link distance is set to be 1 meter for both nodes and $N_T = 2616$ bits. The rate constraint is set to be $(R_1^{\min}, R_2^{\min}) = (1, 0.5)$ Mbit/s. The optimal solution $(\tau^*)^{\text{EE}}$ is $(0.1430, 0.0770)$ in Fig. 4(b). Since the rate demand of user 1 is higher, τ_1^* is approximately twice as τ_2^* .

There are several factors that affect the channel access probability such as the link distance, number of contending nodes, and minimum rate constraint, which we investigate next. Consider two nodes with the same rate constraint fixed to 18 Kbps. We only show the optimal access probability of node 1 as the probabilities are identical for this setting. The distance versus the optimal access probability is depicted in Fig. 4(c). Although τ_1 stays fairly constant up to 7 meters. Beyond this distance, the error probability starts to increase significantly and so does the channel access probability increases exponentially. Fig. 4(d) depicts the effect of the number of nodes on the optimal channel access probability. The rate constraint is fixed to 1 Mbits/sec. The link distances are taken as 1 meter and the number of nodes is varied from two to ten. We observe that the optimal access probability decreases as the number of nodes grows, although the overall system utilization, defined as the sum of individual access probabilities, increases with the number of nodes. Fig. 4(e) shows the optimal access probability versus the rate constraints. The optimal channel access probability increases exponentially to satisfy the rate constraint up to the maximum achievable rate constraint of 1.475 Mbits/s for this scenario.

V. GAME THEORETICAL PERSPECTIVES

Game theory has been widely used in wireless networking for problems such as flow control, power control, routing, and resource sharing can be modeled using game theoretical methods [26]. In this paper, we consider the application of game theory in the energy efficiency of WBANs, based on the framework described in Sections III-IV.

A. Terminology and Nomenclature in Game Theory

Let us first present a brief review of the basics in game theory. The games can be defined in one of the following

two ways: strategic and extensive forms. Consider the strategic form which is defined by the triple

$$\langle \mathcal{K}, \{S_k\}_{k \in \mathcal{K}}, \{u_k\}_{k \in \mathcal{K}} \rangle, \quad (29)$$

where $\mathcal{K} = \{1, 2, \dots, N\}$ is the set of players, S_k is the set of strategies for player k , and u_k indicates the set of utilities for player k . There are three components in a game: players, strategies (actions), utilities (payoffs). The utility or payoff measures the level of satisfaction of the player.

A pure strategy provides a complete definition of how a player will play a game. In particular, it determines the move a player will make for any situation it could face. A player's strategy set is the set of pure strategies available to that player. A mixed strategy is an assignment of a probability to each pure strategy. This allows for a player to randomly select a pure strategy. Since probabilities are continuous, there are infinitely many mixed strategies available to a player.

A non-cooperative game is a game with competition between individual players. The players are selfish and tries to maximize its own utility. When other players' strategies are fixed, the strategy (or strategies) that produces the most favorable outcome for a player is called as the *best response* (BR) of this player. A *Nash Equilibrium* (NE) is a stable state of a system involving the interaction of different participants, in which no participant can gain by a unilateral change of strategy if the strategies of the others remain unchanged. If a profile of actions has the feature that all the players play at their BRs, this profile of actions is a NE for this game.

Since the players are only concerned with their own payoffs, it is often that the NE is not efficient from the viewpoint of the whole system. The famous game, prisoner's dilemma, offers such an example. *Pareto optimality* (PO) can be used to check whether the solution is efficient or not. It is a state of allocation of resources in which it is impossible to make any one individual better off without making at least one individual worse off. The *Social Optimality* (SO) is often used as a measure for the efficiency of a strategy vector, which is defined as the profile that maximizes the weighted sum-utility.

To improve the overall efficiency and enable some level of cooperation in the game, there are two common methods. First method is to provide a recommended strategy by a public signal and let each player choose its action according to its observation of the same public signal (e.g. the traffic light in a traffic game). If no player has any incentive to deviate from the recommended strategy, then it is called as a *Correlated Equilibrium* (CE). For the first method, we can consider that the hub in a star topology provides the public signal using a broadcast frame. The second method is the repeated game in which players participate in repeated interactions within a finite or potentially infinite time horizon. Each player has complete or incomplete information on the history of the game and tries to maximize its expected payoff.

B. Energy Efficiency Game with Two-Users

Consider again the one-hop star network topology in Fig. 5 for two users. We define an energy efficiency game that takes

into account the rate and access probabilities. The strategy of player k is the channel access probability τ_k with the utility function where the energy efficiency is as in (9). This is a game with continuous strategy and can be formulated as a single-stage or repeated game. This assignment of the strategy and utility can be changed according to the specific requirements. We examine the best responses and provide the NE for the single-stage game. The frontier of PO is plotted to check the efficiency of the NE. We show that cooperation is needed to improve the efficiency of the game. Our observations and conclusions can be extended to multiple users.

The best response of node k is its strategy that maximizes its own utility when other players' strategies are fixed. For the game with two nodes, when node 1(2)'s access probability is fixed, the best response of node 2(1) is the access probability that maximizes $u_2 = \eta_2$ ($u_1 = \eta_1$). The results are shown in Fig. 6(a)-(b). By taking the overlap of best responses of two nodes, we obtain the NE of the game that is depicted in Fig. 6(c). We observe that there are multiple NEs for this game and most of them are not efficient. Therefore, the cooperation is necessary for the energy efficiency game. The possible solutions are CE, game with pricing, and repeated games.

In Fig. 6(d), we plot the PO, SO, CE, and NE in the coordinates of normalized energy efficiency. The PO measures the efficiency of the game and any point below the curve of PO is regarded as energy inefficient. We can observe that most of the NEs are not energy efficient. The point of SO, CE, and the most efficient NE point coincide. The SO maximizes the weighted sum utilities and the utilities are equally weighted in Fig. 6(d). The CE is a generalization of the NE, where an arbitrator (public signal) helps the players to correlate their strategies, so as to favor a decision process in the interplay. In Fig. 6, we assume that the public signal is sent by the hub that solves the problem of energy efficiency maximization and broadcasts each user its channel access probability, τ_k .

VI. CHALLENGES AHEAD AND FUTURE DIRECTIONS

A. Future Research Directions

Repeated Games and Incentives: In Section V, a single-stage energy efficiency game has been discussed. A direct extension is to extend it to a multi-stage repeated games where the users are more patient and have discounted utilities. Constructing an equilibrium that gives the players incentive to cooperate and not deviate from this equilibrium is an important research question that closely depends on the protocol and device specific parameters. Energy efficient punishment strategies for cheating player is also an important research area.

Delay requirements and Lyapunov Optimization: While we consider the joint power and data rate requirements for the link adaptation problem in this paper, one can also formulate another joint design objective such as the throughput and delay constraints. The data for delay sensitive applications such as video and voice-over-IP can be prioritized over the delay-insensitive applications such as messaging. There have been several works on formulating the energy efficiency and life-time maximization problems subject to delay and energy constraints

using a stochastic network optimization framework. Open research problems of incorporating rate and delay constraints with interfering links into the problem while maximizing the network energy efficiency still remain as an active research.

Duty Cycling, Sleep Modes, and Energy Consumption Characterization in Sleep Modes: In Section I, we briefly discussed the sleeping patterns and duty cycling. Depending on the devices architecture and application demands, the devices can enter the *deep sleep modes* or *light sleep modes*. On one hand, in the deep sleep mode, the device can turn off multiple components and achieve higher energy savings at the cost of a longer wake-up time. On the other hand, the light sleep mode offers less energy savings at the benefit of a shorter wake-up time. When the device has enough data to transmit, the device can wake up from its deep sleep and transmit its data, while it waits the acknowledgement messages entering the light sleep mode. A major challenge that needs to be addressed to design intelligent MAC protocols with deep and light sleep modes is that the energy consumption of the components of a device need to be characterized precisely in the operation, light sleep, and deep sleep modes so that these values can be incorporated into the MAC protocols. Also, the interoperability between devices from different manufacturers with possibly different device energy consumption need to be taken into account.

Wake-up Radios: Another important research area for energy efficiency is the implementation of WuR-based MAC and routing protocols, and the WuR hardware circuitry design. The WuR radios are extremely useful in applications where events rarely occur but the environment need to be constantly monitored. Devices with WuR capabilities can be active for extended time periods since they can stay in sleep modes longer. However, despite the low power consumption of WuR circuits, their receiver sensitivity is low which limits their communication range. Therefore, extending the communication range of WuRs is a very critical. Also, the false positives in wake-up calls (WuCs) need to be reduced. A WuR employs MAC messages with a flexible address header with specific destinations. Hardware design solutions such as preamble detectors, that filter out the common interference sources and alleviate false wake-up interrupts, are needed to complement the WuR-based MAC and routing protocols.

B. Conclusions and Lessons learned

The energy efficiency of WBANs closely depends on the link distance, channel characteristics, the PHY, MAC, and routing protocols used. This paper has presented two optimal algorithms, CLOEE and EECAP, for energy efficiency maximization in IEEE 802.15.6 IR-UWB WBANs. In CLOEE, a simple but yet optimal algorithm is proposed to determine the frame sizes and number of pulses per burst. EECAP determines optimal channel access probabilities and frame sizes for each node by considering two different energy efficiency models. Based on the simulation results, CLOEE provides significant improvements in terms of energy efficiency (by an order of magnitude) and transmission range (by a factor of two) compared to the static strategies. The EECAP algorithm

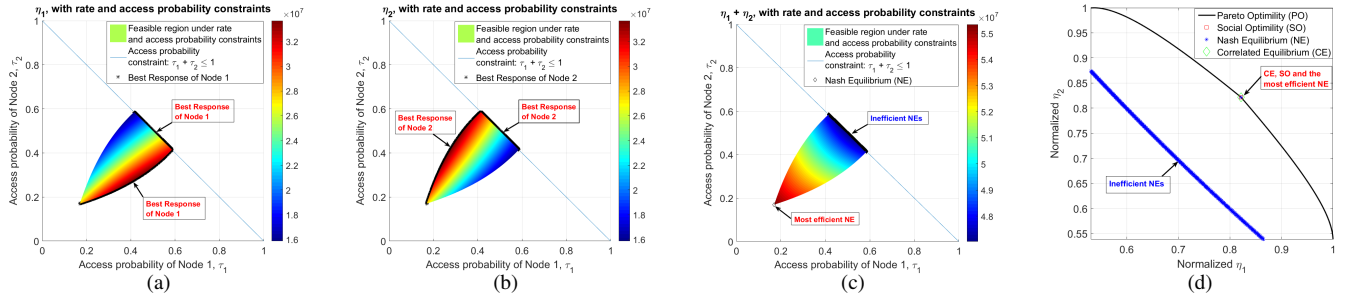


Figure 6. (a)-(b) Best responses of Node 1 and Node 2, (c) Nash Equilibrium (NE) of single-stage energy efficiency game, and (d) Efficiency evaluation of Pareto Optimality (PO), Social Optimality (SO), Correlated Equilibrium (CE) and Nash Equilibrium (NE).

finds the optimal access probability and frame size efficiently. We note the following take away messages for link adaptation:

- For longer link distances, due to the lower SNR and thereby higher error probability, shorter frames sizes and more pulses per burst should be preferred, whereas in shorter link distances, longer frames sizes and few pulses per burst can significantly increase the energy efficiency since the link is more reliable.
- The optimal access probability increases with the link distance, increases exponentially with the minimum rate constraint, and decreases logarithmically with the number of nodes.

ACKNOWLEDGMENT

Yang Liu's participation in this publication was made possible by NPRP grant #6-415-3-111 from the Qatar National Research Fund (a member of Qatar Foundation). The statements made herein are solely the responsibility of the authors.

REFERENCES

- [1] *IEEE Standard for Local and Metropolitan Area Networks, Part 15.6: Wireless Body Area Networks*, IEEE Std. 802.15.6-2012 Std., Feb. 2012.
- [2] K. Davaslioglu, Y. Liu, and R. D. Gitlin, "CLOEE - Cross-Layer Optimization for Energy Efficiency of IEEE 802.15.6 IR-UWB WBANs," in *Proc. IEEE GLOBECOM*, Dec. 2016, pp. 1-7. [Online]. Available: arXiv:1609.05256v1 [cs.NI]
- [3] Y. Liu, K. Davaslioglu, and R. D. Gitlin, "Energy Efficiency Optimization of Channel Access Probabilities in IEEE 802.15.6 UWB WBANs," in *Proc. IEEE Wireless Communications and Networking Conference (WCNC)*, March 2017. [Online]. Available: arxiv.org/abs/1610.02092
- [4] H. Karvonen, J. Iinatti, and M. Hämäläinen, "A cross-layer energy efficiency optimization model for WBAN using IR-UWB transceivers," *Telecommun. Systems*, vol. 58, no. 2, pp. 165-177, Feb 2015.
- [5] M. S. Mohammadi, Q. Zhang, E. Dutkiewicz, and X. Huang, "Optimal frame length to maximize energy efficiency in IEEE 802.15.6 UWB Body Area Networks," *IEEE Wireless Commun. Lett.*, vol. 3, no. 4, pp. 397-400, Aug 2014.
- [6] M. S. Mohammadi, E. Dutkiewicz, Q. Zhang, and X. Huang, "Optimal energy efficiency link adaptation in IEEE 802.15.6 IR-UWB body area networks," *IEEE Wireless Commun. Lett.*, vol. 18, no. 12, pp. 2193-2196, Dec 2014.
- [7] W. Ye, J. Heidemann, and D. Estrin, "Medium access control with coordinated adaptive sleeping for wireless sensor networks," *IEEE/ACM Trans. Network.*, vol. 12, no. 3, pp. 493-506, June 2004.
- [8] R. Jurdak, A. G. Ruzzelli, and G. M. P. O'Hare, "Adaptive radio modes in sensor networks: How deep to sleep?" in *Proc. IEEE Conf. Sensor, Mesh and Ad Hoc Communications and Networks (SECON)*, June 2008, pp. 386-394.
- [9] R. Jurdak, A. G. Ruzzelli, and G. M. P. O'Hare, "Radio sleep mode optimization in wireless sensor networks," *IEEE Transactions on Mobile Computing*, vol. 9, no. 7, pp. 955-968, July 2010.
- [10] C. Tachatzis *et al.*, "An energy analysis of IEEE 802.15.6 scheduled access modes," in *Proc. IEEE GLOBECOM Workshops (GC Wkshps)*, Dec 2010, pp. 1270-1275.
- [11] C. Tachatzis *et al.*, *Revised Selected Papers in Third International ICST Conference Ad Hoc Networks (ADHOCNETS) 2011*. Springer Berlin Heidelberg, 2012, ch. An Energy Analysis of IEEE 802.15.6 Scheduled Access Modes for Medical Applications, pp. 209-222.
- [12] K. S. Deepak and A. V. Babu, "Optimal packet size for energy efficient WBAN under m-periodic scheduled access mode," in *Proc. Twentieth National Conf. Commun. (NCC)*, Feb-March 2014, pp. 1-6.
- [13] C. S. Lin and P. J. Chuang, "Energy-efficient two-hop extension protocol for wireless body area networks," *IET Wireless Sensor Systems*, vol. 3, no. 1, pp. 37-56, March 2013.
- [14] A. Manjeshwar and D. P. Agrawal, "TEEN: A routing protocol for enhanced efficiency in wireless sensor networks," in *Proc. IEEE Int. Parallel and Distributed Processing Symposium (IPDPS)*, April 2001, pp. 2009-2015.
- [15] A. Manjeshwar and D. P. Agrawal, "APTEEN: A hybrid protocol for efficient routing and comprehensive information retrieval in wireless," in *Proc. IEEE Int. Parallel and Distributed Processing Symposium (IPDPS)*, April 2002, pp. 8 pp-.
- [16] J. Polastre, J. Hill, and D. Culler, "Versatile low power media access for wireless sensor networks," in *Proc. Inf. Conf. Embedded Networked Sensor Systems (SenSys)*, 2004, pp. 95-107.
- [17] A. G. Ruzzelli, G. M. P. O'Hare, and R. Jurdak, "Merlin: Cross-layer integration of mac and routing for low duty-cycle sensor networks," *Ad Hoc Netw.*, vol. 6, no. 8, pp. 1238-1257, Nov. 2008.
- [18] S. Gezici, H. Kobayashi, H. V. Poor, and A. F. Molisch, "Performance evaluation of impulse radio UWB systems with pulse-based polarity randomization," *IEEE Transactions on Signal Processing*, vol. 53, no. 7, pp. 2537-2549, July 2005.
- [19] K. Witrisal *et al.*, "Noncoherent ultra-wideband systems," *IEEE Signal Process. Mag.*, vol. 26, no. 4, pp. 48-66, July 2009.
- [20] R. D. Gitlin, J. F. Hayes, and S. B. Weinstein, *Data Communications Principles*. New York, N.Y.: Springer, 1992.
- [21] T. Wang, W. Heinzelman, and A. Sedy, "Link energy minimization in IR-UWB based wireless networks," *IEEE Trans. Wireless Commun.*, vol. 9, no. 9, pp. 2800-2811, September 2010.
- [22] P. P. Mercier *et al.*, *Ultra-Low-Power Short-Range Radios*. New York: Springer, 2015, ch. Pulsed Ultra-Wideband Transceivers, pp. 233-280.
- [23] M. S. Bazaraa, H. D. Sherali, and C. M. Shetty, *Nonlinear Programming: Theory and Algorithms*. New York, NY: John Wiley & Sons, Ltd, 1993.
- [24] "Channel model for Body Area Network (BAN)," IEEE P802.15 Working Group for Wireless Personal Area Networks (WPANs), Tech. Rep. IEEE P802.15-08-0780-09-0006, April 2009.
- [25] L. Giarr, G. Neglia, and I. Tinnirello, "Medium access in WiFi networks: Strategies of selfish nodes," *IEEE Signal Process. Mag.*, vol. 26, no. 5, pp. 124-127, 2009.
- [26] A. B. MacKenzie and L. A. DaSilva, *Game theory for wireless engineers*. Synthesis Lectures on Communications, 2006, vol. 1, no. 1.